X-ray Emission from Electron Betatron Motion in a Laser-Plasma Accelerator

G. R. Plateau[*,†], C. G. R. Geddes[*], D. B. Thorn[**], N. H. Matlis[*], D. E. Mittelberger[*], T. Stoehlker[‡], M. Battaglia[*], T. S. Kim[*], K. Nakamura[*], E. Esarey[*] and W. P. Leemans[*]

[*]*LOASIS Program at LBNL, Berkeley, CA 94720, USA*
[†]*École Polytechnique, Palaiseau, 91128, France*
[**]*EMMI at GSI, Darmstadt, 64291, Germany*
[‡]*APIX at GSI, Darmstadt, 64291, Germany*

Abstract. Single-shot x-ray spectra from electron bunches produced by a laser-plasma wakefield accelerator (LPA) [1, 2] were measured using a photon-counting single-shot pixelated Silicon-based detector [3], providing for the first time single-shot direct spectra without assumptions required by filter based techniques. In addition, the electron bunch source size was measured by imaging a wire target, demonstrating few micron source size and stability. X-rays are generated when trapped electrons oscillate in the focusing field of the wake trailing the driver laser pulse [4, 5, 6, 7, 8]. In addition to improving understanding of bunch emittance and wake structure, this provides a broadband, synchronized femtosecond source of keV x-rays. Electron bunch spectra and divergence were measured simultaneously and preliminary analysis shows correlation between x-ray and electron spectra. Bremsstrahlung background was managed using shielding and magnetic diversion.

Keywords: x-ray, betatron motion, laser-plasma accelerator
PACS: 41.75.Jv, 52.38.-r, 52.38.Kd, 52.65.Rr

INTRODUCTION

Laser-plasma accelerators (LPAs) rely on the excitation of an electron density wave by a laser in a plasma, whose longitudinal field accelerates electrons [1, 2]. Capillary-guided LPAs have demonstrated high-quality electron bunches at 1 GeV [9] with 2.5% *r.m.s.* energy spread. LPAs have a broad range of applications such as free-electron lasers [10], THz [11, 12] and x-ray radiation sources [4, 5]. In the self-trapping regime, LPAs rely on the transverse wavebreaking effects [13] of highly nonlinear waves [14] to inject electrons into the accelerating phase of the electron density wave. Conventionally, keV x-rays are produced by injecting multi-GeV electron bunches into permanent magnetic undulators, typically of centimeter- or millimeter-scale periods. The wakefield generated behind the driver laser pulse in an LPA acts as a strong focusing channel in which off-axis injected electrons undergo oscillations, typically of submilliliter period, suitable for generating collimated keV x-ray radiation [4, 5, 15, 16, 8] from sub-GeV electron bunches.

In this paper, the first direct single-shot x-ray spectra from betatron motion of electrons produced by an LPA, along with bunch size measurements, are presented. Single-shot spectra and shot-integrated spectra were collected with a pixelated Silicon-based detector in single-photon counting mode, providing detailed x-ray spectra. An x-ray shadow of crossed thin wires, acting as knife edges, shows that the electron bunch size in the wakefield is smaller than the spot size and stable shot-to-shot, in reasonable agreement with simulations considering the limited magnification. Moreover, it is shown that x-ray spectral amplitude is correlated with the accelerator performance by measuring simultaneously electron and x-ray spectra for two regimes of the accelerator. Shielding and apertures were used to ensure both good control of Bremsstrahlung background, due to secondary collisions of low energy background electrons, and collimation of the measured x-ray beam.

EXPERIMENTAL SETUP AND THEORETICAL CONCEPTS

In the LOASIS facility at the Lawrence Berkeley National Laboratory, an 800-nm laser pulse was focused (7.2 μm FWHM intensity spot size) into Hydrogen gas ($\sim 3 \times 10^{19}$ e^-/cm^3) from a 2.2 mm inner diameter supersonic

CP1299, *Advanced Accelerator Concepts: 14th Workshop*, edited by S. H. Gold and G. S. Nusinovich

nozzle. The 0.45 J, 45 fs FWHM, linearly polarized laser pulse was produced using a 10 Hz Ti:Al_2O_3 chirped-pulse amplification laser system. Single-shot diagnostics were used (Fig. 1) to characterize the electron bunches generated including an integrating current transformer (ICT) for the total electron bunch charge, and a magnetic dipole spectrometer for the electron bunch energy distribution [17]. To measure broadband electron energy distributions, two charge-calibrated screens at 45 degrees from each other were used, leaving a "gap" in the distribution at the separation between the two screens.

Simultaneously, x-ray emission from betatron motion of the electrons in the plasma wave was measured using a back-illuminated charge coupled device (CCD) camera, which had a 1024×256 pixel chip, with 26 μm square pixels, a 40 μm depletion region of Silicon, a 1–5 μm dead Si layer, and a measured resolution of 0.23 keV FWHM. The camera, which required a cooling system, had its own vacuum pump and was coupled to the LPA vacuum chamber with a stainless steel beam pipe and a window. The window was made of 0.1 μm of Aluminum, 14 μm of polycarbonate, 18 μm of Kapton, and 25 μm of Beryllium. Bremsstrahlung radiation, resulting from secondary collisions of low energy electrons inside the target chamber and from stopping of higher energy electrons in the magnetic dipole spectrometer, was mitigated by enclosing the x-ray CCD camera with lead bricks, and by placing high-density polyethylene (HDPE) plates inside the target chamber (Fig. 1).The stainless steel coupling pipe had a rectangular cross-section (1×0.25 inch) to match the size of the CCD chip and thereby limit the solid angle of acceptance. HDPE plates inside the target chamber were placed so as to limit further the solid angle of acceptance. In addition, two sets of crossed wires (12.5 μm and 50 μm diameter), made of Gold-plated Tungsten fibers, opaque to < 10 keV x-rays (shown later in Fig. 3), were placed 22 cm downstream from the gas jet and imaged onto the x-ray CCD camera, 220 cm downstream from the gas jet, providing a measure of the transverse electron bunch in the plasma wave.

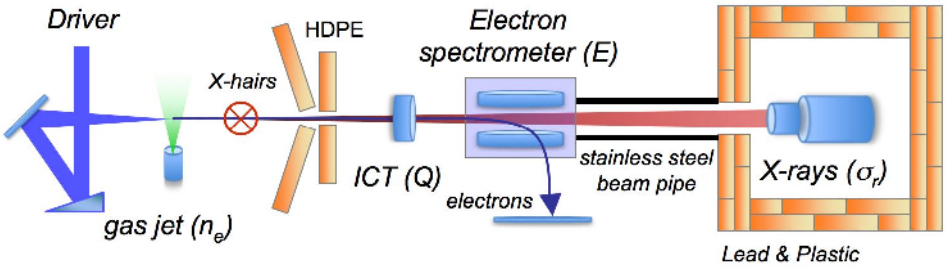

FIGURE 1. Schematic of the experimental setup. The driver laser beam is focused using an off-axis parabolic mirror onto a supersonic gas jet of neutral electron density n_e. Charge (Q), energy (E) distribution, and source size (σ_r) can be monitored. Bremsstrahlung background is controlled using high-density polyethylene (HDPE) and lead bricks.

Esarey *et al.* [15] provide a theoretical description of betatron x-ray radiation in plasma-focusing channels. A driver laser pulse, with normalized vector potential $a_0 \propto \sqrt{I}$, where I is the laser intensity, drives a plasma wave. In the self-injection regime, in which the present experiments operated, very high wakefield amplitudes are generated leading to wavebreaking and self-injection of background electrons. In this regime, injection occurs continually as the laser propagates into fresh plasma resulting in Boltzmann-type electron energy distributions, with large energy spreads [18]. During its acceleration the electron bunch resides in the nearly uniform ion channel formed behind the driver laser pulse. The strong transverse focusing field associated with the ion channel, which diameter is typically much greater than the bunch radius, induces oscillations of the electron bunch at the betatron wavelength $\lambda_\beta = \lambda_p\sqrt{2\gamma} \propto \sqrt{\gamma/n_e}$, where γ is the relativistic factor of the electron, λ_p is the plasma wavelength, and n_e is the plasma density. At a plasma density of 3×10^{19} e^-/cm^3 and for typical electron energy distributions ranging from ~ 10 to ~ 100 MeV, $\lambda_p \simeq 6\mu$m, $\gamma \sim 20$–200, and $\lambda_\beta \sim 38$–120 μm. This betatron motion induces directional synchrotron radiation within a cone of angle $\theta \simeq a_\beta/\gamma$, where $a_\beta \simeq 1.33 \times 10^{-10}\sqrt{\gamma n_e}\sigma_r$ is the betatron strength parameter, and σ_r is the distance from the edge of the electron bunch to the laser propagation axis. Information on the electron bunch size, σ_r, is provided by measuring the cut-off frequency of the x-ray spectrum, given by $\hbar\omega_c$ [keV] $\simeq 1.1 \times 10^{-4}\gamma^2 n_e$ [10^{19} e^-/cm^3] σ_r [μm]. For typical parameters such as a 40 MeV electron bunch, an electron density of 3×10^{19} e^-/cm^3, and an electron bunch radius of 1μm, $\hbar\omega_c \simeq 2$ keV.

EXPERIMENTAL RESULTS

Experimental parameters were chosen so as to operate the accelerator in two stable regimes, referred to as "high regime" and "low regime", where the first delivered higher charge electron bunches and x-ray yield than the second (Fig. 2).

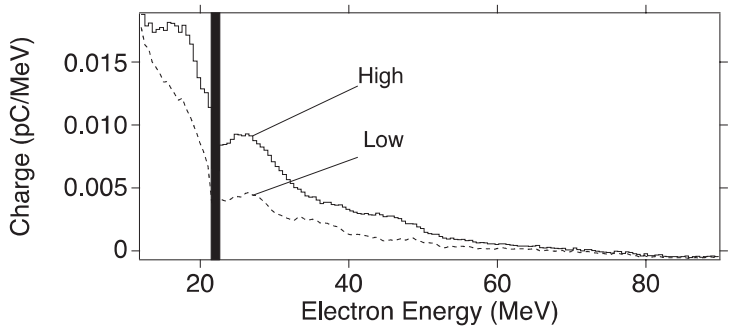

FIGURE 2. Average electron distributions (200 shots) for a "high regime" with high charge, high x-ray yield (*solid curve*), and for a "low regime" with lower charge, lower x-ray yield (*dashed curve*). The mask region at 22 MeV is the region not viewed by the spectrometer due to its mechanical and optical design.

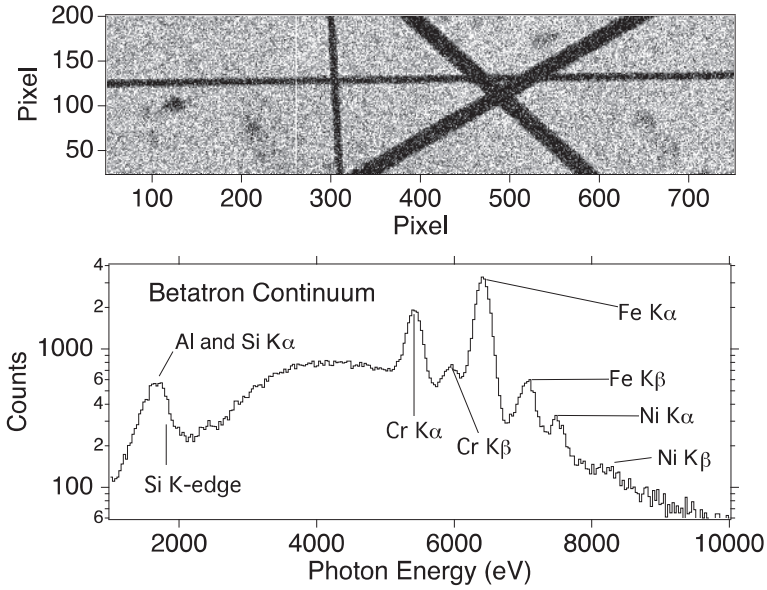

FIGURE 3. Accumulated image (*top*) and spectrum (*bottom*) considering only single pixel absorption events, acquired in the high regime, of 200 shots. The top image shows the shadows of the ten times magnified 12.5 and 50 μm crossed wires used for estimating the transverse electron bunch size at the source. The continuum part of the accumulated spectrum corresponds to the betatron emission. The K-shell fluorescence lines are due to secondary electron collisions with beam line components.

After background subtraction, single-shot x-ray spectra were calculated by generating a histogram of the image acquired by the CCD camera. In this paper, only single pixel absorption events (SPAE) were considered. An SPAE is an isolated x-ray hit on the CCD, for which surrounding pixels level do not exceed the background level. Thus, the number of counts in a pixel for an SPAE is directly proportional (3.65 eV/count) to the energy of the absorbed x-ray. With this method the spectral information is dependent on the flux of x-rays. If every pixel is illuminated (100% occupancy image) there is no SPAE, hence no spectral information. In these experiments, a single-shot image contained $\sim 1.6 \times 10^5$ photons ($\sim 60\%$ occupancy), leading to $\sim 10^3$ SPAE and direct measurement of x-ray spectra. In addition, to verify the accuracy of the SPAE method to depict spectral features, a 5 μm Titanium filter was placed

in front of the camera in the high regime. The predicted reduction of x-ray intensity by the Ti 4.97 keV K-edge was observed, validating the SPAE method.

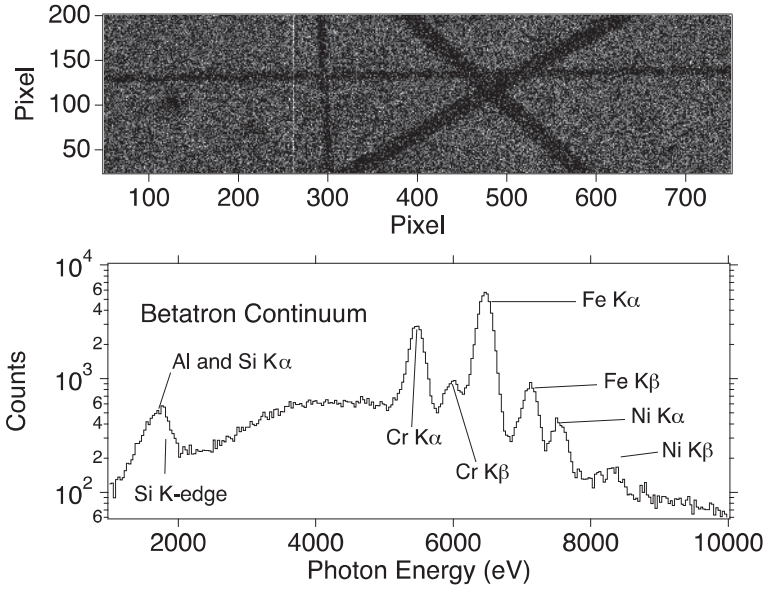

FIGURE 4. Accumulated image (*top*) and spectrum (*bottom*) considering only single pixel absorption events, acquired in the low regime, of 200 shots. The top image shows the shadows of the ten times magnified 12.5 and 50 μm crossed wires used for estimating the transverse electron bunch size at the source. The continuum part of the accumulated spectrum corresponds to the betatron emission. The K-shell fluorescence lines are due to secondary electron collisions with beam line components.

Measured amplitudes of the x-ray spectra were correlated with the accelerator performance as illustrated in Fig. 3 and Fig. 4 which were respectively acquired in the high and low regime. The K-shell fluorescence lines from x-rays generated by electron collisions with the stainless steel (Fe, Cr, Ni) vacuum coupling pipe, as well as Al K-shell and Si K-shell fluorescence lines from the window and the CCD dead layer, provided shot-to-shot calibration of the energy scale of the x-ray spectra and showed no fluctuations within the CCD resolution (0.23 keV), verifying again the detection technique. For the first time, single-shot direct x-ray spectra were measured from a laser-plasma accelerator. Using this technique, spectra have enough counts to allow single-shot calculation of the x-ray cut-off frequency (Fig. 5) and verify, within the limits of the CCD window transmission (> 3 keV), the theoretical shape of the betatron x-ray spectra [15] that filter based techniques assume.

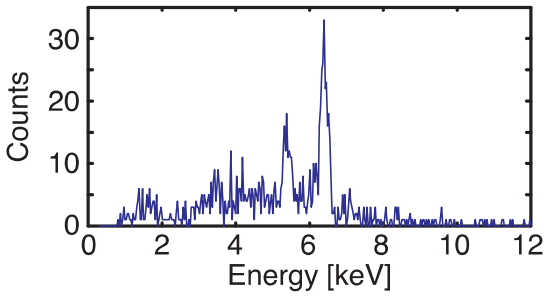

FIGURE 5. Example of single-shot x-ray spectrum from a laser-plasma accelerator. The K-shell fluorescence lines, due to secondary electron collisions with beam line components, provide shot-to-shot calibration of the energy scale. The continuum part peaks at about 4 keV.

The transverse radiation source size was determined by imaging two sets of crossed wires made of Gold-plated Tungsten fibers, opaque to < 10 keV x-rays (Fig. 4). Both sets were placed 22 cm downstream of the gas jet, to optimize their magnification ($\times 10$) on the x-ray CCD camera, while ensuring that the absorption of energy left in the laser after its interaction with the plasma would not damage the cross hairs. For an x-ray emission angle greater than

the angular cross-section of the wire, the upper limit of the transverse radiation source size is determined by the ratio of the wire shadow edge width and the magnification. In these experiments, this condition was strongly satisfied with an emission angle > 6 mrad and an angular cross-section of $\simeq 0.11$ mrad for the 50 μm diameter wire. Analysis of the data of Figure 3 showed the electron bunch source size in the wakefield was at most 6 ± 3 μm in both planes, which includes laser pointing fluctuation over 200 shots and a limited resolution of $\simeq 2.6$ μm. Simulations predicted < 2 μm.

CONCLUSION

In conclusion, single-shot direct spectral measurements of betatron radiation from an LPA using a sensitive state-of-the-art pixelated x-ray CCD camera were successfully achieved for the first time. Detector and analysis method (single shot absorption events) were shown to provide high resolution, reliable single-shot spectral information, demonstrating generation of high flux ($\sim 1.6 \times 10^5$ photons in a 1.5×6 mrad collection angle) x-ray beams by an LPA. Using a knife-edge technique, x-ray imaging was used to measure the shot-integrated electron bunch source size ($< 6 \pm 3$ μm). Simultaneous measurement of charge, electron energy and divergence distributions, and x-ray spectra were demonstrated. Preliminary correlation of the x-ray spectra with the accelerator performance was observed by operating the accelerator in two distinct regimes, relative high and low charge of the generated electron bunch.

ACKNOWLEDGMENTS

The authors gratefully acknowledge contributions from Cs. Tóth, M. Chen, E. Cormier-Michel, C. B. Schroeder, and J. van Tilborg. This work was supported by the Director, Office of Science, Office of High Energy Physics, of the U.S. Department of Energy under Contract No. DE-AC02-05CH11231 and NA-22.

REFERENCES

1. T. Tajima, and J. M. Dawson, *Phys. Rev. Lett.* **43**, 267–270 (1979).
2. E. Esarey, C. B. Schroeder, and W. P. Leemans, *Rev. Mod. Phys.* **81**, 1229–1285 (2009).
3. W. Fullagar, J. Uhlig, M. Walczak, S. Canton, and V. Sundstrom, *Review of Scientific Instruments* **79**, 103302 (2008), URL `http://link.aip.org/link/?RSI/79/103302/1`.
4. P. Catravas, E. Esarey, and W. P. Leemans, *Meas. Sci. Tech.* **12**, 1828–1834 (2001).
5. A. Rousse, K. T. Phuoc, R. Shah, A. Pukhov, E. Lefebvre, V. Malka, S. Kiselev, F. Burgy, J.-P. Rousseau, D. Umstadter, and D. Hulin, *Phys. Rev. Lett.* **93**, 135005–135008 (2004).
6. W. P. Leemans, E. Esarey, J. van Tilborg, P. A. Michel, C. B. Schroeder, C. Tóth, C. G. R. Geddes, and B. A. Shadwick, *IEEE Trans. Plasma Sci.* **33**, 8 (2005).
7. K. T. Phuoc, F. Burgy, J.-P. Rousseau, V. Malka, A. Rousse, R. Shah, D. Umstadter, A. Pukhov, and S. Kiselev, *Physics of Plasmas* **12**, 023101 (2005), URL `http://link.aip.org/link/?PHP/12/023101/1`.
8. F. Albert, R. Shah, K. T. Phuoc, R. Fitour, F. Burgy, J.-P. Rousseau, A. Tafzi, D. Douillet, T. Lefrou, and A. Rousse, *Phys. Rev. E* **77**, 056402 (2008).
9. W. P. Leemans, B. Nagler, A. J. Gonsalves, Cs. Tóth, K. Nakamura, C. G. R. Geddes, E. Esarey, C. B. Schroeder, and S. M. Hooker, *Nature Physics* **2**, 696 – 699 (2006).
10. C. B. Schroeder, W. M. Fawley, F. Gruner, M. Bakeman, K. Nakamura, K. E. Robinson, C. Toth, E. Esarey, and W. P. Leemans, *AIP Conference Proceedings* **1086**, 637–642 (2009), URL `http://link.aip.org/link/?APC/1086/637/1`.
11. W. P. Leemans, C. G. R. Geddes, J. Faure, Cs. Tóth, J. van Tilborg, C. B. Schroeder, E. Esarey, G. Fubiani, D. Auerbach, B. Marcelis, M. A. Carnahan, R. A. Kaindl, J. Byrd, and M. C. Martin, *Phys. Rev. Lett.* **91**, 074802 (2003).
12. J. van Tilborg, C. B. Schroeder, Cs. Tóth, C. G. R. Geddes, E. Esarey, and W. P. Leemans, *Phys. Rev. Lett.* **96**, 014801 (2006).
13. S. V. Bulanov, F. Pegoraro, A. M. Pukhov, and A. S. Sakharov, *Phys. Rev. Lett.* **78**, 4205–4208 (1997).
14. C. B. Schroeder, E. Esarey, and B. A. Shadwick, *Phys. Rev. E* **72**, 055401 (2005).
15. E. Esarey, B. A. Shadwick, P. Catravas, and W. P. Leemans, *Phys. Rev. E* **65**, 056505 (2002).
16. K. T. Phuoc, S. Corde, R. Shah, F. Albert, R. Fitour, J.-P. Rousseau, F. Burgy, B. Mercier, and A. Rousse, *Phys. Rev. Lett.* **97**, 225002 (2006).
17. K. Nakamura, W. Wan, N. Ybarrolaza, D. Syversrud, J. Wallig, and W. P. Leemans, *Review of Scientific Instruments* **79**, 053301 (2008), URL `http://link.aip.org/link/?RSI/79/053301/1`.
18. C. B. Schroeder, E. Esarey, B. A. Shadwick, and W. P. Leemans, *Phys. Plasmas* **13**, 033103 (2006).